International Journal of Science and Research (IJSR)
ISSN (Online): 2319-7064
Index Copernicus Value (2015): 78.96 | Impact Factor (2015): 6.391

Theoretical Approach to the Corrosion Inhibition of Some Imidazoline Derivatives on Iron Surface Using Molecular Dynamic Simulations and Quantum Chemical Calculations

Kelechi Uwakwe[1], Anthony Obike[1, 2], Louis Hitler[3]

[1]Corrosion and Electrochemistry Research Group, Department of Pure & Applied Chemistry, University of Calabar, Calabar, Nigeria

[2]Department of Pure & Industrial Chemistry, Abia State University, Uturu, Abia State, Nigeria

[3]CAS Key Laboratory for Nanosystem and Fabrication, CAS Centre for Excellence in Nanoscience National Centre for Nanoscience and Technology University of Chinese Academy of Sciences, Beijing, China

Abstract: ***Molecular dynamic (MD) simulations and quantum chemical calculations were used to study the adsorption and inhibitive effect of (Z)-2-(2-(henicos-12-en-1-yl)-4,5-dihydro-1H-imidazol-1-yl) ethan-1-amine (HNED and 2-(2-((10Z 13Z)-nonadeca-10,13-dien-1-yl)-4,5-dihydro-1H-imidazol-1-yl)-ethan-1-ol (NDDI) on iron at333 K and 353K using different chemical parameters. The results show the imidazoline ring to lay out plainly with the iron surface, with the molecules having different geometry structures at the different temperatures studied. The active sites for adsorption of these molecules were shown to be the N=C-N region on the imidazoline ring, the double bonded carbons atom at the hydrophobic tail and the rarely nitrogen and oxygen heteroatoms. Considering both the molecular dynamic simulation and the quantum chemical calculations, the order for the inhibitive/adsorption effect is given as NDDI > HNED at geometry optimization, NDDI > HNED at 333 K and HNED > NDDI at 353 K. Theoretically NDDI is more preferred based on the results obtained using their geometry optimized structures. The molecules are said to be physically adsorbed on the iron surface.***

Keywords: Iron, Corrosion, Molecular dynamic simulations, Quantum chemical calculation, Imidazoline derivatives.

1. Introduction

Metals and their alloys, most especially iron is used widely in industrial fields. The corrosion of metals lead to huge financial losses and many potential safety issues [1]. As a protection technique, the addition of corrosion inhibitor is a very good way to keep metals and their alloys away from corrosion from the environment [2]. Most corrosion inhibitors are mainly organic compound which slow down the corrosion process of a metal through the mechanism of adsorption [3] which is influenced by factors such as steric effect, electronic structure, aromaticity, electron density at the donor atoms and p-orbital character of the donating electrons [4]. Amines and their salts are said to be the most economic and effective corrosion inhibitors for oil and gas wells [5]. Imidazoline is a typical amine-nitrogen compound which is heterocyclic in nature. Heterocyclic organic compounds consisting of a π-system or heteroatoms such as N, S, or O are said to be good corrosion inhibitors and are used to prevent the deterioration of metals [6]. The lone electron pairs of electron in the hetero atoms and the planarity of a molecule are important features that determine the adsorption of molecules on the metallic surface [7]. Organic compounds also have heteroatoms such as nitrogen, oxygen, Sulphur and phosphorous in their aromatic or long chain system. The presence of these heteroatoms and suitable functional groups can trigger the adsorption of the inhibitor on the metal surface and are mostly assumed to be the active sites of a particular molecule [8].

Theoretical studies at molecular level have been reported to aim at gaining insight on the molecules chemical activities [9] and mostly in the study of the corrosion inhibition processes [10] considering model molecules and their structural and electronic properties. This includes quantum chemical calculations which have proven to be a very useful and powerful tool for studying the mechanism of corrosion inhibition [11].There is a strong relationship between the corrosion inhibition efficiencies/adsorption ability of most compounds with several quantum chemical parameters such as the works reported on Vinyl imidazole derivatives [12], Triazoles and Benzimidazole derivatives [13], Shift bases [14] and some Quinoxaline derivatives [15] just to mention a few. The quantum chemical principle is a very useful tool in predicting the inhibition potential of structurally related organic compound [16]. Molecular dynamic simulation gives a better understanding of how inhibitor molecules behave on a metal surface. Molecular dynamic study is very important for understanding structural changes, interactions and energetics of molecules which can greatly enhance our ability to control the essential interfacial properties of a system in a wide variety of problems e.g. corrosion. As such the adsorption of inhibitor molecule on surfaces has recently become the subject of intensive investigation in the study of corrosion [17].

In this study two imidazoline derivatives consisting mainly of the 'head' (heterocyclic ring), the 'anchor' (or 'pendant') the substituent attached to the heterocyclic ring and the 'tail' (the long alkyl hydrophobic tail) [18]wereinvestigated. Molecular dynamic simulation was performed to simulate the adsorption and to determine the modes of adsorption of these imidazoline derivatives on iron surface in a vacuum/gas phase in order to understand the interactions

between these molecules and the Fe surface. The interaction energy, binding energy, bond length and natural atomic charge have all been calculated for each of the dynamic structures obtained from the molecules at the two temperatures studied. Quantum chemical calculations were performed in the vacuum/gas phase at 333 K and 353K. Parameters such as dipole moment (μ), energy of deformation (D) van der waals accessible area (Λ), highest occupied molecular orbital energy (E_{HOMO}), lowest unoccupied molecular orbital (E_{LUMO}), energy gap (ΔE), absolute electro negativity (χ), electron affinity (A), ionization potential (I), global hardness (η), global softness (S), number of electron transfer (ΔN) and Fukui function $f(r)$were calculated to determine the active adsorption sites of the imidazoline molecules. The chemical structures of the compounds studied are shown in Table 1.

Table 1: Name, chemical formula, abbreviation, structure and molecular weight of the imidazoline derivatives

Name	*Chemical formula*	*Abbreviation*	*Structure*	*Molecular weight(g/mol)*
(Z)-2-(2-(henicos-12-en-1-yl)-4,5-dihydro-1H-imidazol-1-yl) ethan-1-amine	$C_{26}H_{51}N_3$	HNED	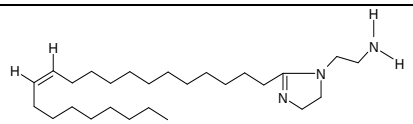	405.70
2-(2-((10Z,13Z)-nonadeca-10,13-dien-1-yl)-4,5-dihydro-1H-imidazol-1-yl) ethan-1-ol	$C_{24}H_{44}N_2O$	NDDI	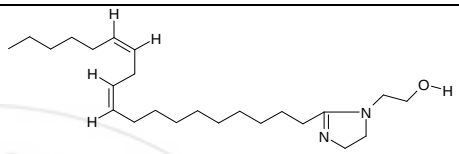	376.60

2. Computational Details

This study was performed using Material Studio softwaredeveloped byAccelyrs Incorporation San Diego California. This software is a high-quality quantum mechanics computer program. This study employed three modules as described on the Accelrys website and they are Forcite module (an advanced classical molecular mechanical tool that allows fast energy calculations and reliable geometry optimization of molecules and periodic system), Vamp module (a semi empirical molecular orbital package for molecular organic and inorganic system) [19] and Dmol³ module (a program which uses the density functional theory (DFT) with a numerical radial function basis set to calculate the electronic properties of molecule cluster surface and crystalline solid materials from the first principle [20]. In this study the molecules were sketched, the hydrogens were adjusted and the molecules were cleaned using sketch tool available in the material visualizer.

The molecular dynamic simulation was done using the forcite module in a simulation box of dimension (20.1Å × 8.6Å ×34.4Å) with periodic boundary conditions to model a representative part of the interface devoid of any arbitrary effects. The box consists of an iron slab and a vacuum layer of height 28.1Å. The Fe crystals was cleaved along the (001) plane with the uppermost layer released and the inner layer fixed.

The MD simulation was performed at temperatures of 333K and 353K respectively. The number of particle and the volume of each system in the ensemble are constant and the ensemble has a well-defined temperature (NVT Ensemble) with a time step of 0.1fs and simulation time of 5ps to show the effect of change in temperatures on the molecule properties. The value of the interaction energy of the molecules and the Fe (001) surface was calculated according to the following equation [21]

$$E_{Fe\ -\ molecule} = E_{complex} - E_{Fe} - E_{molecule} \quad (1)$$

Where $E_{Fe\ -\ molecule}$ is the interaction energy, $E_{complex}$ is the total energy of the Fe crystal together with the adsorbed inhibitor molecule, E_{Fe} is the total energy of the Fe crystal and $E_{molecule}$is the total energy of the inhibitor molecule.

The binding energy is the negative energy of the interaction energy and it is given as

$$E_{Binding} = -E_{Fe\ -\ molecule} \quad (2)$$

For the whole simulation procedure, the force field CVFF (Consistent Valence Force Field) was used. It is mainly used for the study of structures and binding energy, though it can also predict vibrational frequencies and conformation energy reasonably well.

In order to further clarify the adsorption mechanism of the selected molecules quantum chemistry calculations were performed using two modules which are Vamp and Dmol³ modules. Using the Vamp module, theoretical calculations were carried out at the Restricted Hartree-Fock level (RHF) using the Hamiltonian parametric method 3 (PM3) which is based on the neglect of diatomic differential overlap (NDDO) approximation. The BLYP (from the name Becke for the exchange part and Lee, Yang and parr for the correlation part) functional method was used using the Dmol³ module via DNP basic set. The Dmol³ uses the density functional theory (DFT). DFT has provided a very useful tool for understanding molecular properties and for describing the behavior of atoms in molecules. DFT methods have become very popular in the last decade due to their accuracy and shorter computational time. DFT has been found to be successful in providing insights into chemical reactivity and selectivity, in terms of global parameters such as electro negativity (χ), hardness (η), and softness (S), and local ones such as the Fukui function $f(r)$ and local softness $s(r)$. Thus, for an N-electron system with total electronic energy E and an external potential $v(r)$, the chemical potential μ, known as the negative of the electro negativity χ, has been defined as the first derivative of E with respect to N at constant external potential v(r) [22]

$$\chi = -\gamma = -\left(\frac{\partial E}{\partial N}\right)_{v(r)} \quad (3)$$

Hardness (η) has been defined within DFT as the second derivative of E with respect to N at constant external potential $v(r)$ [22]

$$\eta = \left(\frac{\partial^2 E}{\partial N^2}\right)_{v(r)} = \left(\frac{\partial \gamma}{\partial N}\right)_{v(r)} \quad (4)$$

The number of electrons transferred (ΔN) from the inhibitor molecule to the metal surface can be calculated by using equation (5) [23]

$$\Delta N = \frac{\chi_{Fe} - \chi_{mole}}{[2(\eta_{Fe} + \eta_{mole})]} \quad (5)$$

where $\chi_{Fe}$and χ_{mole} denote the absolute electro negativity of iron and the molecule, respectively, and $\eta_{Fe}$and η_{mole} denote the absolute hardness of iron and the molecule, respectively. In this study, we use the theoretical value of χ_{Fe}=7.0 eV and η_{Fe} = 0 for the computation of number of transferred electrons [23]. The difference in electronegativity drives the electron transfer, and the sum of the hardness parameters acts as a resistance [24]. Electron affinity (A) and ionization potential (I)are related in turn to the energy of the highest occupied molecular orbital (E_{HOMO}) and of the lowest unoccupied molecular orbital (E_{LUMO}) using equations (6) and (7) [25]

$$I = -E_{HOMO} \quad (6)$$

$$A = -E_{LUMO} \quad (7)$$

Electronegativity (χ) is the measure of the power of an atom or group of atoms to attract electrons towards itself [26] and according to Koopman's theorem, electronegativity and global hardness is related to the electron affinity (A) and ionization potential (I) according to equation (8) and (9)

$$\chi = \frac{I+A}{2}, \quad \chi = -\frac{E_{LUMO} + E_{HOMO}}{2} \quad (8)$$

$$\eta = \frac{I-A}{2}, \quad \eta = -\frac{E_{LUMO} - E_{HOMO}}{2} \quad (9)$$

According to Yang and Parr, 1985 Global softness (S) can also be defined as the reciprocal of the global hardness as shown according to equation (10)

$$S = \frac{1}{\eta} \quad (10)$$

The local reactivity of the imidazoline molecules was analyzed through evaluation of the Fukui indices [27]. The Fukui indices are measures of chemical reactivity, as well as an indicative of the reactive regions and the nucleophilic and electrophilic behavior of the molecule. Regions of a molecule where the Fukui indices is large are chemically softer than regions where the Fukui indices is small, and by invoking the hard and soft acids and bases (HSAB) principle in a local sense, one may establish the behavior of the different sites with respect to hard or soft reagents. The Fukui function $f(r)$ is defined as the first derivative of the electronic density $\rho(r)$ with respect to the number of electrons N at constant external potential $v(r)$. Thus, using a scheme of finite difference approximations from Mullikan population analysis of atoms in MOP and depending on the direction of electron transfer, we have [27].

$$f^-(r) = \rho_N(r) - \rho_{N-1}(r) \quad (11) \text{ electrophilic attack}$$

$$f^+(r) = \rho_{N+1}(r) - \rho_N(r) \quad (12) \text{ nucleophilic attack}$$

Wheref^-, f^+, ρ_{N+1},ρ_N, and $\rho_{N-1}$are the Fukui negative, Fukui positive, electronic densities of anionic, electronic densities of neutral and electronic densities of cationic species, respectively.

The N corresponds to the number of electrons in the molecule. $N+1$ corresponds to an anion, with an electron added to the LUMO of the neutral molecule while $N-1$ corresponds to the cation with an electron removed from the HOMO of the neutral molecule. All calculations in this study were done on the structures at geometry optimized, at333K and at 353K. The colour codes for the atoms in the molecules studied are gray for carbon, blue for nitrogen, red for oxygen and white for hydrogen. And the atoms have been numbered (FIG 2) for an in depth understanding of the role played by each of the atoms present in the molecules

3. Results and Discussions

3.1 Molecular dynamic simulation

An adsorption model containing one imidazoline derivative molecule at a time and Fe surface was built using the Materials Studio software, and the simulation was performed using theForcitemodule resulting in the modes of adsorption of the imidazoline derivatives at geometry optimization, 333 K and 353K on iron surface. These are shown in Fig.1a and 1b. Equilibration of the system is established by the steady average values of energy as well as temperature [21]. The close contacts between the inhibitor molecules and iron surface as well as the best adsorption configurations for the compounds are shown in Fig.1. The calculated interaction and binding energy obtained from the molecular dynamics simulation are shown in Table 2. According to the modes of adsorption of the three (3) imidazoline derivatives on Fe (001) surface it is observed that the head group of the imidazoline molecule is mostly attached plainly to the metal surface while the alkyl hydrophobic tail deviates from the metal surface consequently preventing the surface from H_2O. In this way, the exposed part of Fe surface can be reduced by the covering of the inhibitor molecules, consequently creating a barrier between the surface of the metal and the corrosive agents [28].

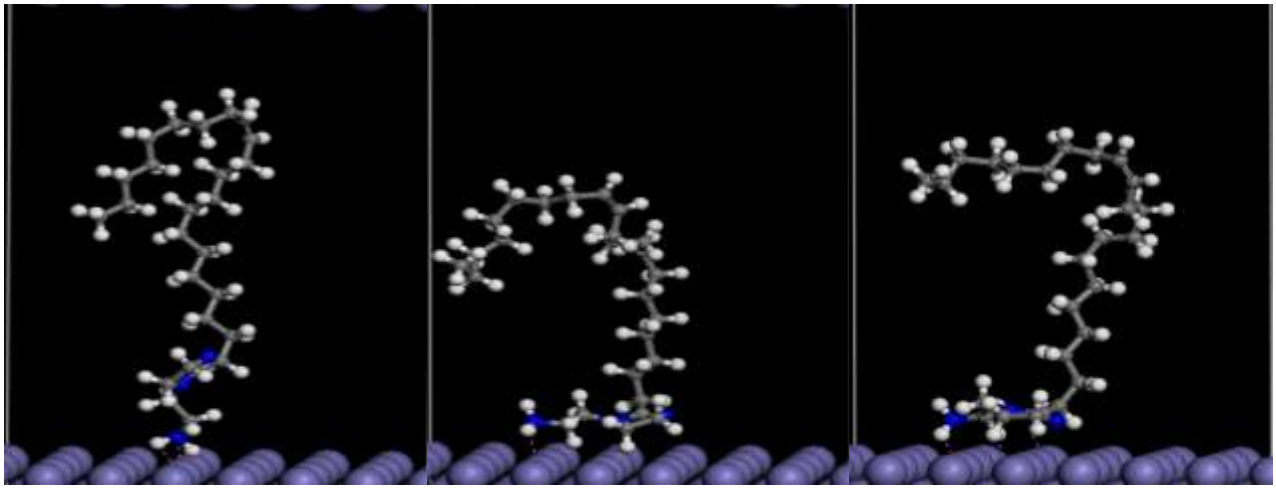

(i) (ii) (iii)

Figure 1: (a) Modes of adsorption of HNED at (i) geometry optimization (ii) 333 K and (iii) 353 K

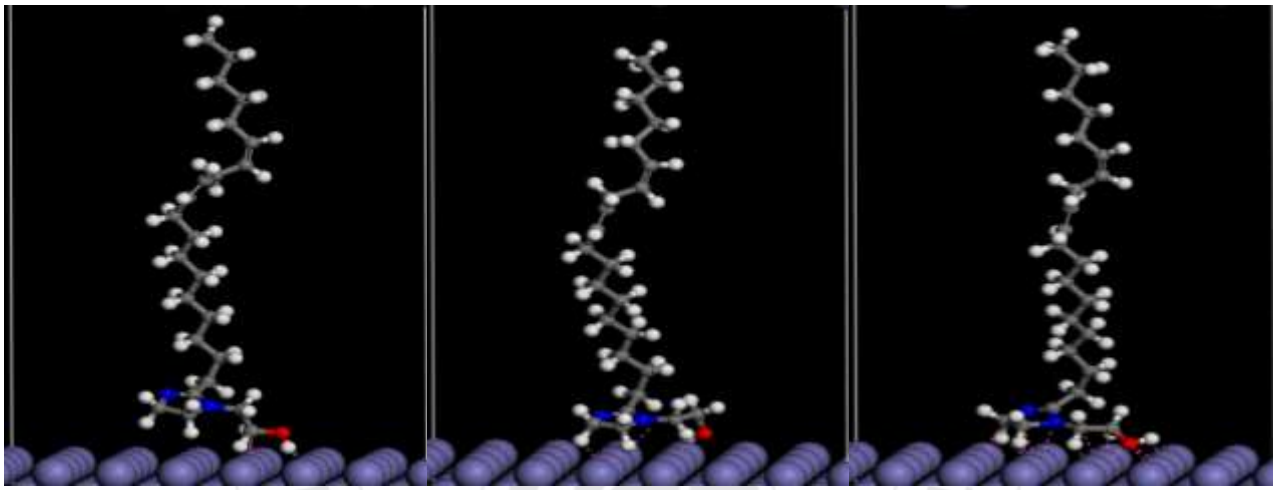

(i) (ii) (iii)

Figure 1: (b) Modes of adsorption of NDDI at (i) geometry optimization (ii) 333 K and (iii) 353 K

The values of the interaction energies are shown in Table 2, the two molecules show very low interaction energy at the two temperatures studied. The more negative the interaction energy the more it can effectively interact with the iron surface and the higher the binding energy and the inhibition efficiency. It is seen that all the molecules studied have a positive binding energy. The larger the value of the binding energy, the stronger the bonding between the molecules and the iron surface, the easier the molecules is adsorbed on the iron surface and thus the higher the inhibitor efficiency. NDDI shows the lowest interaction and highest binding energy at 333 K, while HNED shows the lowest interaction and highest binding energy at 353 K.

3.1.1 Geometry optimized structures, equilibrium geometry structures and energies of HNED and NDDI

The geometry optimized structures and the equilibrium structures of HNED and NDDI are shown in Fig. 2. At geometry optimization, the system is said to be at the minimum energy state. The entropy of the molecules at geometry optimization can be said to be equal to zero. At equilibrium (333K and 353K) the entropy of the molecules increases due to temperature. The geometry of the molecules at equilibrium is brought about when the temperature and the energy of the system/molecules reach a balance [21]. It is also observed that the energy at geometry optimization is lower than the energy at equilibrium for each molecule as seen in table 2. This is because the temperature at equilibrium increases the entropy of the atoms in the molecule which leads to an increase in the energy of the system (molecule). Thus, the geometry optimized structures is said to be the most stable structure.

3.1.2 Minimum Distance between Fe surface and imidazoline molecules

Table 2 shows the Minimum distance between each of the adsorbed imidazoline derivatives and the Fe surface at equilibrium (333 K and 353 K). From Table 2 it is seen that 3.078 Å to 3.410 Å are the minimum distance range observed between the imidazoline derivatives and the Fe surface. Due to the high distance value ($d > 3$ Å) [29, 30] observed between the imidazoline molecules and the Fe surface, it suggests the imidazoline molecules are physically adsorbed on the Fe surface.

Table 2: Interaction, binding, molecular energy and distance between Fe surface and the imidazoline derivatives of HNED and NDDI

	Interaction Energy (Kcal/mol)			*Binding Energy (Kcal/mol)*			*Molecular Energy (Kcal/mol)*			*Distance (Å)*	
		333 K	*353 K*		*333 K*	*353 K*	*Geo Opt*	*333 K*	*353 K*	*333 K*	*353 K*
HNED		-151	-191		151	191	74	166	171	3.398	3.329
NDDI		-192	-150		192	150	60	167	143	3.078	3.410

Figure 2: Structures of HNED and NDDI at Geometry optimization, 333 K and 353 K

3.1.3 Bond length analysis

Figure 3 shows the bond length in Armstrong unit (Å) for the geometry optimized and equilibrium structures of the molecules. It is observed that changes in the structural orientation of the atoms in the molecules at different temperatures bring about a change in the bond length of each of the atom in the molecule from each other. This clearly shows that at the two temperatures studied the inhibitors assume different conformations (Fig. 2). The changing structures of these inhibitor molecules at the two temperatures studied also reveals an effect on bond angles by torsional strain. It is clearly seen that atoms which are connected by double bonds shows shorter bond length than the ones connected by single bonds which is a known fact in chemistry. Energy of a certain value has to be supplied in order to break any bond. This means that the closer the nuclei of the bonding atoms are a greater supply of energy is needed to separate the atoms due to large force of attraction between the atoms. In other words, short bond length requires high dissociation energies to break the bond. From Fig. 3 it is observed that the heteroatoms (nitrogen and oxygen) bonded to a carbon atom show a shorter bond length than the carbon to carbon bond length at geometry optimized and at equilibrium (333 K and 353 K) structures. It means that more energy will be required to break this bond and hence a high chemical reactivity. The shorter the bond length the higher the bond energy and the higher is the reactivity of the bond.

3.1.4 Natural atomic charge

From conventional chemical theory, all chemical interactions can be by electrostatic or orbital interactions. Electrostatic interaction is propelled by the presence of electric charge on the molecule involved. Local electric charges have been proven to be very important in several chemical reactions as well as physiochemical characteristics of compounds [21]. Fig. 4shows the natural atomic charges in coulombs (C) for the imidazoline derivative molecules at geometry optimization as well as at equilibrium structures. It is observed that the atoms possess negative charges except for C8 carbon atom in HNED and NDDI. This may be due to inductive effect between the carbon atom and the N4 and N7 nitrogen atoms in HNED and NDDI knowing that the C8 carbon atom is between two highly negatively charged nitrogen atoms. The C-N bond is strongly polarized towards the nitrogen atom and this can lead to high dipole moment.

It was also observed that the charges become more negative at equilibrium structures from the geometry optimized structures. The hetero atoms involved (oxygen and nitrogen) are more negative than the carbon atoms for all the molecules studied except for the last carbon atom at the tail end of the molecules, this may be due to dipole moment (uneven distribution of charges) observed between the last carbon atom and the last hydrogen atom. The oxygen atom was found to be more negative than the nitrogen atoms in NDDI. The hydrogen atoms present in the imidazoline molecules are all positively charged.

Molecule	*Geometry Optimization*	*Equilibrium Structure at 333 K*	*Equilibrium Structure at 353 K*
HNED		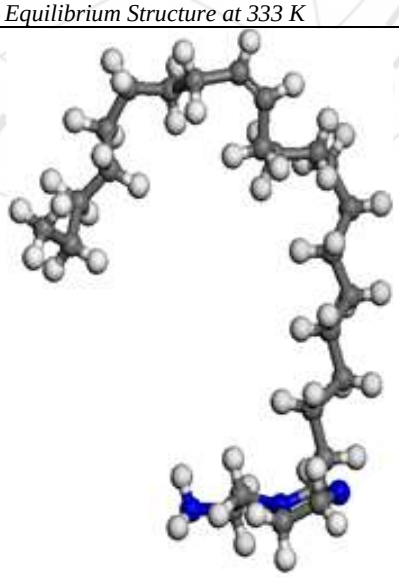	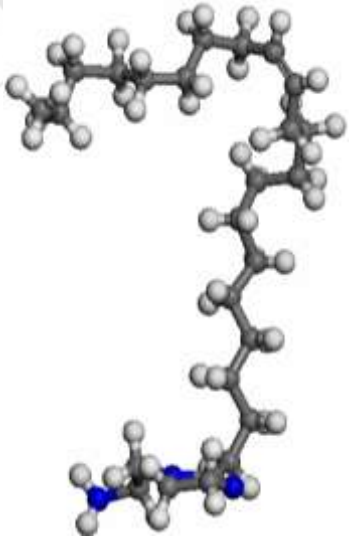

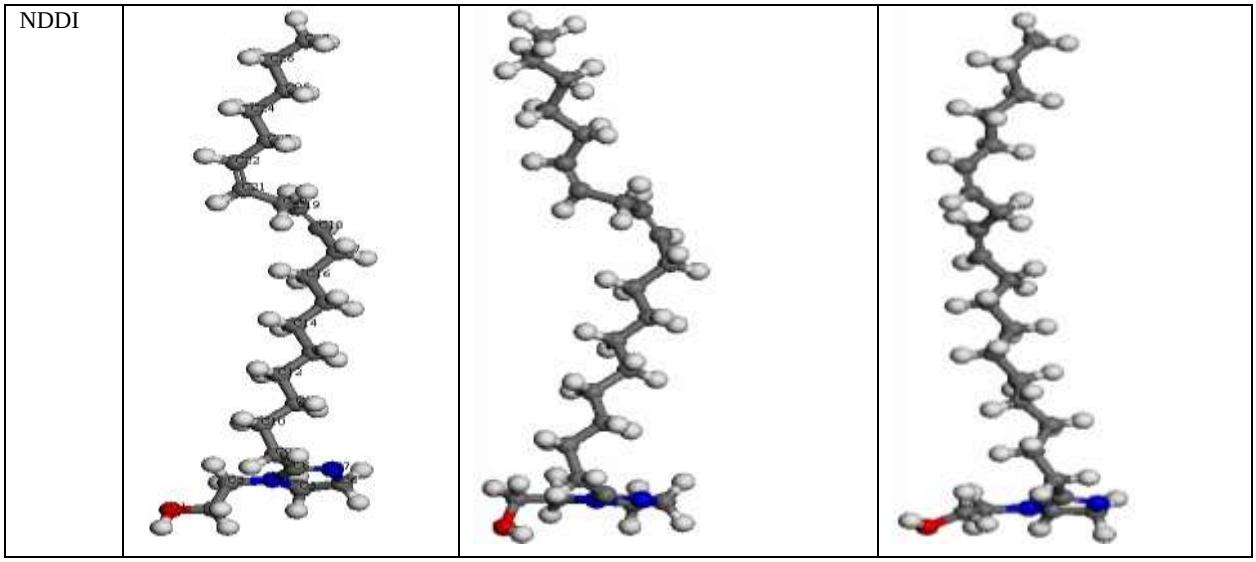

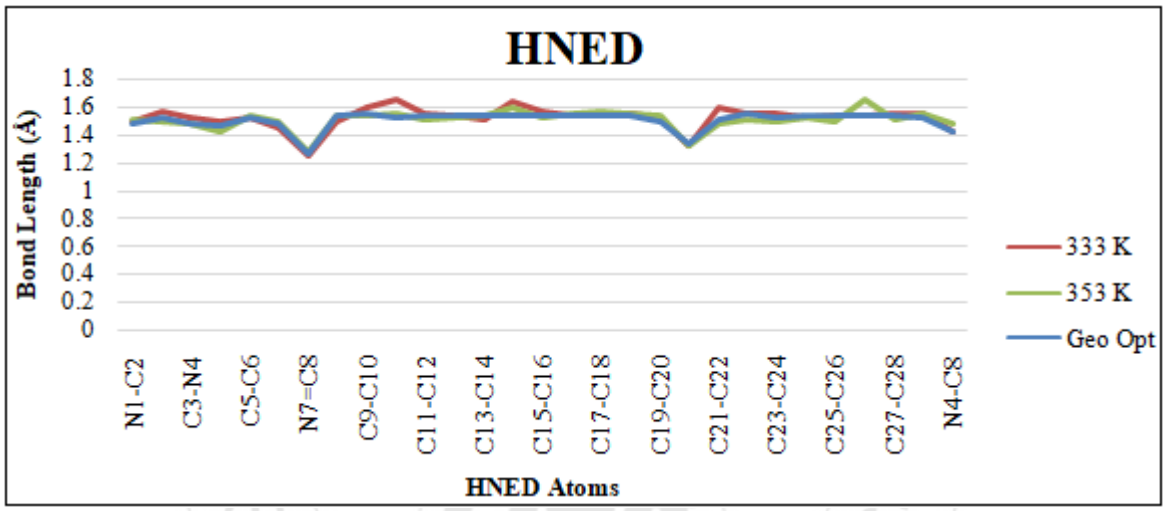

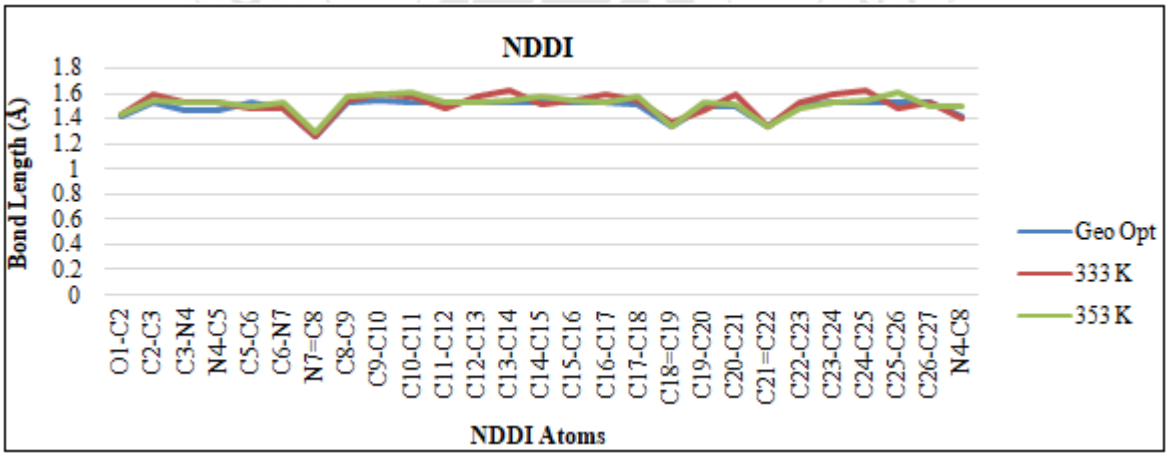

Figure 3: Bond length analysis for HNED and NDDI at Geometry Optimization, 333 K and 353 K

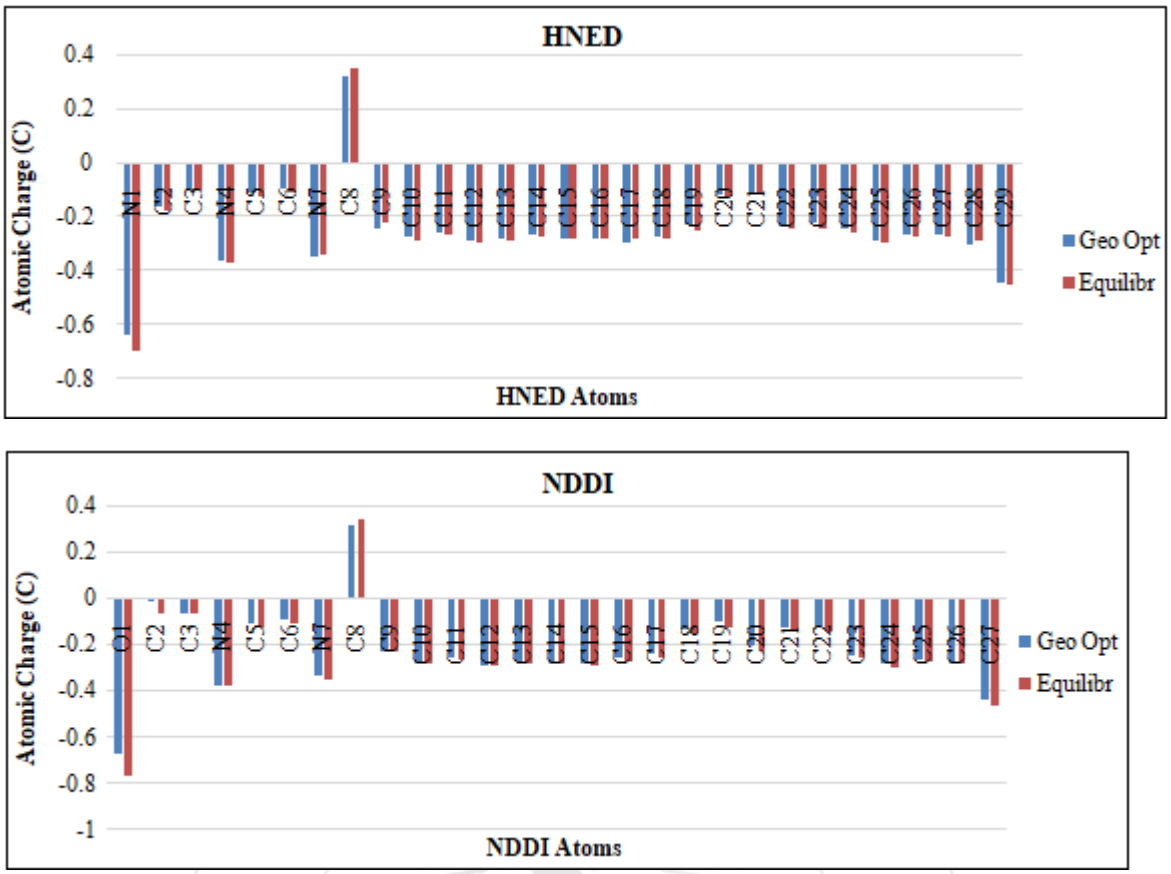

Figure 4: Natural atomic charge for HNED and NDDI at Geometry optimization and at equilibrium

3.2 Quantum chemistry calculation

To further understanding the interactions between the two molecules and the iron surfaces, the quantum chemical calculation was performed. The computed quantum chemical properties such as energy of highest occupied molecular orbital (E_{HOMO}), energy of lowest unoccupied molecular orbital (E_{LUMO}), energy gap (ΔE), dipole moment (μ), energy of deformation (D), van der waal accessible area (Λ), electro negativity (χ), electron affinity (A), ionization potential (I), global hardness (η), global softness (S), andthe fraction of electrons transferred from the inhibitor to iron surface (ΔN), are shown in Table 3.

Table 3: Calculated quantum chemical parameters for HNED, NDDI and HDDE

	HNED			*NDDI*		
Quantum parameter	*Geo Op*	*333 K*	*353 K*	*Geo Op*	*333 K*	*353 K*
E_{HOMO}(eV)	-4.200	-4.234	-4.078	-4.312	-4.219	-4.172
E_{LUMO} (eV)	0.174	0.017	-0.242	-0.266	-0.389	-0.293
ΔE gap (eV)	4.374	4.251	3.836	4.086	3.830	3.879
μ (Debye)	4.298	4.331	4.069	3.448	3.866	3.549
D (eV)	2603.3	2237.6	2520.1	1706.8	1830.2	1641.7
A (eV)	-0.174	-0.017	0.242	0.266	0.389	0.293
I (eV)	4.200	4.234	4.078	4.312	4.219	4.172
Λ (Å^2)	611.8	599.3	607.1	556.9	553.9	558.0
χ (eV)	2.01	2.11	2.16	2.27	2.30	2.23
η	2.19	2.13	1.92	2.04	1.92	1.94
S	0.46	0.47	0.52	0.49	0.52	0.52
ΔN	1.140	1.148	1.260	1.159	1.224	1.229

The frontier molecular orbital (FMO) theory is often used to predict the adsorption centers of inhibitor molecules which are responsible for the interaction with the metal surface atoms [31-33]. According to the frontier molecular orbital theory, the formation of a transition state is due to an interaction between the frontier orbital which are highest occupied molecular orbital (HOMO) and lowest unoccupied molecular orbital (LUMO) of reactants. The HOMO is known to be the orbital that could act as an electron donor while the LUMO is known to be the orbital that could act as the electron acceptor [33]. The widely-accepted concept about the inhibitor adsorption mechanism is that: the higher the HOMO energy, the greater the tendency of offering electrons to the metal surface atoms, and the higher the inhibitive/adsorption effect. Similarly, the lower the LUMO energy, the greater the tendency of accepting electrons from the metal surface atoms, and the better inhibitive/adsorption effect [32, 34]. From Table 3 HNED is seen to have the highest HOMO energy at geometry optimization and at 353 K, while NDDI has the highest HOMO energy at 333 K meaning that these molecules can give out electrons to the vacant d-orbital of the Fe atom more efficiently at their respective state. The negative signs observed on the values of E_{HOMO} shows that the adsorption is physisorption [35]. This is in line with the assumption made concerning the distance observed between molecules and the Fe surface (Table 2) that the adsorption observed by the molecules on the Fe surface may be physisorption. From Table 3 also NDDI shows the lowest LUMO energy at geometry optimization, 333 K and 353 K meaning that this molecule can accept electron from the d-orbital of the Fe atom more efficiently at the respective states, resulting in the creation of another bond and also the greater the amount of energy that will be released due to the addition of an electron to the molecule (electron affinity). The FMO theory also gives an

explanation of the energy gap ($\Delta E=E_{LUMO} - E_{HOMO}$) which is a important parameter that is used to characterize the molecule's stability in chemical reactions, a decrease in the energy gap usually leads to easier polarization of the molecule, and that is the basis which the concept of ''activation hardness" has been defined on [31, 36]. It is widely accepted that smaller energy gap ΔE means better adsorption ability hence better inhibitive efficiency because the energy to remove an electron from the last occupied orbital will be low [4]. From Table 3 it is observed that NDDI shows a smaller energy gap at geometry optimization and at 333 K, while HNED shows a smaller energy gap at 353 K. This is in agreement with the binding energy results obtained from the molecular dynamic simulation section in Table 2.

Fig 5shows the HOMO and LUMO orbital plot on the imidazoline molecules, it can be observed that the HOMO location in the molecules is mostly distributed on the imidazoline ring and few of the plot is observed in pendent group joined to the imidazoline ring in HNED and NDDI, this is familiar to the preferred sites for electrophilic attack (f^-), we can say that the part of the molecules with high HOMO density will be oriented toward the iron surface as seen in Fig 1, and the adsorption could be by sharing the lone pair of electrons of nitrogen atom and the π electrons of the aromatic ring with the Fe surface [37]. The LUMO which gives the preferred sites for nucleophilic attack (f^+) is mainly located around the double bonded carbon atoms in the alkyl hydrophobic tail in HNED and NDDI. Note that the blue and yellow isosurface depict the electron density difference; the blue regions show electron accumulation, while the yellow regions show electron loss.

Total dipole moments as well as energy of deformability are parameters characterizing the interaction between molecules [21]. Dipole moment tells us about the charge separation in a molecule. The larger the difference in electronegativity of bonded atoms the larger the dipole moment [38]. Deformation energy on the other hand is the energy required to change the orientation of a molecule. From Table 3 NDDI shows a lower dipole moment at geometry optimization and at 333 K and HNED shows a lower dipole moment at 353 K. Molecule with lower dipole moment has been reported to show good inhibitive/adsorption effect [39]. Meanwhile some works has also shown that molecules with higher dipole moments have been shown to have good inhibition efficiency [1, 40]. Therefore, the dipole moment is not a significant factor in concluding the expected trend in adsorption. Ionization energy is a fundamental descriptor of the chemical reactivity of atoms and molecules. High ionization energy indicates high stability and chemical inertness and low ionization energy indicates high reactivity of the atoms and molecules [12]. HNED has the least value of ionization energy at geometry optimization and at 353 K while NDDI has the least value of ionization energy at 333 K. Electron affinity of an atom or molecule is defined as the amount of energy released when an electron is added to a neutral atom or molecule in the gaseous state to form a negative ion [41]. NDDI has the largest amount of energy release at geometry optimization, 333 K and 353 K. Table 3also shows the van der Waal accessible surface for HNED and NDDI at geometry optimization, 333 K and 353 K. HNEDhave a larger surface area than NDDI. This seems to have no effect in the adsorption ability of the molecules owing to the fact that NDDI has a better adsorption ability at geometry optimization and at 333 K. It may also be that the larger a molecule is the more its accessible surface area. The difference in surface area at geometry optimization, 333 K and 353 K may be due to the change in the configuration of these molecules at different temperatures as observed from FIG 2.

Another important property to measure the molecular stability as well as reactivity of a molecule is the absolute hardness and softness. Chemical hardness fundamentally suggests the resistance towards the deformation or polarization of the electron cloud of the atoms, ions or molecules under small perturbation of chemical reaction. A hard molecule has a large energy gap and a soft molecule has a small energy gap [42]. From Table 3, NDDI at geometry optimized structure and at 333 K while HNED at 353 K shows the lowest hardness and the highest softness. Normally, the molecule with the least value of global hardness (hence the highest value of global softness) is expected to have the highest adsorption/inhibitive ability [43] this is also in line with the binding energy and the energy gap results. For the simplest transfer of electron, adsorption could occur at the part of the molecule where softness(S), which is a local property, has a highest value [37].

The electronegativity values of the two molecules at geometry optimization, 333 K and 353 K are shown in Table 3. When two system, Fe and inhibitor are brought together, electrons will flow from lower χ(inhibitor) to higher χ(Fe) until the chemical potentials become equal [12]. From Table 3 it is observed that the two molecules show lower χ values compared to χ(Fe) which is 7.0ev, that means that electrons will flow more freely from the inhibitor molecule to the metal surface. The fraction of electron transfer (ΔN) is brought about by the difference in electronegativity in the molecules which drives the electron transfer divided by two times the sum of the hardness parameter of the molecules and the iron surface [23]. These values are calculated and presented in Table 3. Values of ΔN shows that the adsorption ability resulting from electron donation agrees with Lukovits's study [43], that is if $\Delta N < 3.6$, the adsorption ability increases by increasing electron donating ability of these molecules to donate electrons to the metal surface. The result indicates that ΔN values is in line with the binding energy results obtained in the molecular dynamic section and the energy gap results. Higher fraction of electron transfer indicates better inhibition efficiency and from Table 3 NDDI shows the highest number of electron transfer at geometry optimization and at 333 K, while HNED shows the highest number of electron transfer at 353 K.

To determine the active site of a molecule, three influencing and controlling factors: natural atomic charge, distribution of frontier molecular orbital and Fukui indices have to be considered [21]. Local reactivity is analyzed by means of the condensed Fukui function. Condensed Fukui functions allow us to distinguish each part of the molecule on the basis of its distinct chemical behaviour due to the different substituent

functional groups [12]. The nucleophilic and electrophilic attack is controlled by the maximum values of f^+ and f^-. The calculated Fukui indices for nucleophilic and electrophilic attack for the three selected inhibitors are tabulated in Table 4 (only C, N, and O are quoted) and their active sites are plotted in Figures 5. It can be seen from Table 4 that the largest values of f^-considering the geometry optimized molecular structures are located on the N7 and N4 atoms (mainly the N=C-N region) located on the ring for both HNED and NDDI, which indicates that these two atoms prefer to form a chemical bond by donation of electrons to the metal surface. While the largest values of f^+ are located on the C8 and N7 atoms in HNED and C22, C18, C19 and C21 atoms for NDDI, which further suggest that these atoms will be responsible to form a back bond by the acceptance of electron from the metal surface. It is observed that the atoms mentioned for the electrophilic and nucleophilic attack are bonded to each other and are seen to have a shorter bond length as observed from the bond length analysis, this confirms that the double bond and a shorter bond length have a role to play in the inhibitive/adsorption ability of a molecule. But the particular atom which is more susceptible to electrophilic and nucleophilic attack in each of the molecules at geometry optimization and at the two temperatures studied is the atom with the highest Fukui indices value [44, 45] and these values are boldly highlighted in Table 4. For HNED and NDDI the N7 atom is the most susceptible atom for electrophilic attack, while the C8 atom for HNED and the C22 atom for NDDI is the most susceptible atom for nucleophilic attack based on the geometry optimized structure.

Molecule	*HOMO Orbital Plot*	*LUMO Orbital Plot*	*Sites for Electrophilic Attack (f⁻)*	*Sites for Nucleophilic Attack (f⁺)*
HNED	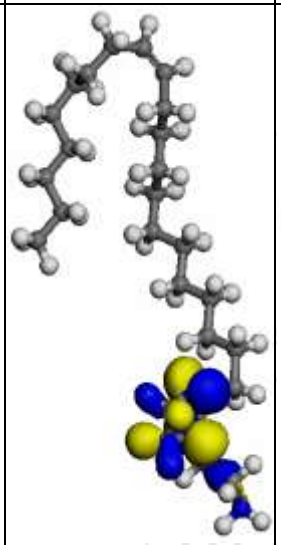	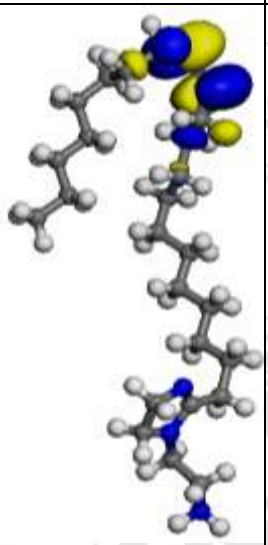		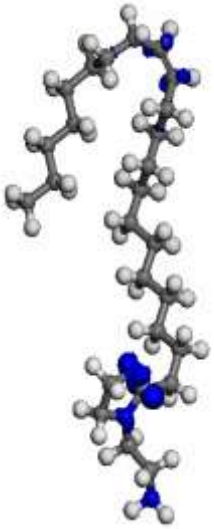
NDDI	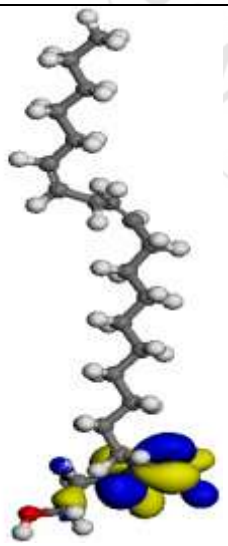	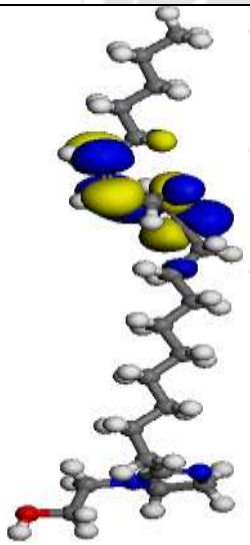	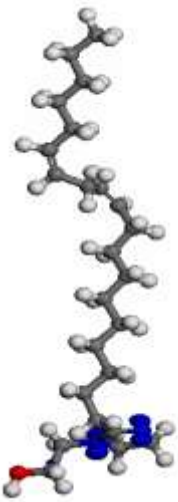	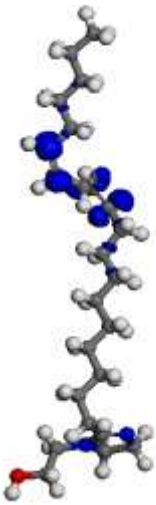

Figure 5: HOMO and LUMO Orbital plots, Electrophilic and Nucleophilic attack plots at Geometry Optimization for HNED and NDDI

Table 4: Fukui indices (f^- and f^+) values for (a) HNED and (b) NDDI

(a)

	f^-			f^+		
Atom	*Geo Opt*	*Equilibrium*		*Geo Opt*	*Equilibrium*	
		333 K	*353 K*		*333 K*	*353 K*
O1	0.020	0.036	0.016	-0.001	0.005	0.008
C2	-0.007	-0.013	-0.006	0.000	0.001	-0.001
C3	-0.038	-0.052	-0.025	-0.001	0.000	-0.005
N4	0.148	0.117	0.142	0.000	0.000	0.020
C5	-0.042	-0.037	-0.042	-0.001	-0.002	-0.012
C6	-0.037	-0.040	-0.033	-0.001	-0.001	-0.010
N7	**0.173**	**0.188**	**0.170**	-0.002	0.003	0.093
C8	0.027	0.038	0.035	-0.001	0.000	**0.115**
C9	-0.017	-0.015	-0.019	-0.002	-0.001	-0.010
C10	-0.014	-0.022	-0.019	-0.002	-0.002	-0.011
C11	-0.007	-0.001	-0.002	-0.003	-0.006	-0.005
C12	-0.006	-0.015	-0.005	-0.003	-0.001	-0.005
C13	-0.004	-0.008	-0.002	-0.005	-0.003	-0.005
C14	-0.003	0.004	-0.004	-0.007	-0.017	-0.004
C15	-0.003	-0.003	-0.001	-0.008	-0.010	-0.009
C16	-0.002	-0.003	-0.001	-0.023	-0.022	-0.017
C17	-0.001	-0.003	-0.003	-0.030	-0.024	-0.012
C18	-0.005	-0.005	-0.005	0.106	**0.122**	0.035
C19	0.004	0.005	0.005	0.052	0.071	-0.002
C20	0.000	-0.001	-0.001	-0.049	-0.042	-0.028
C21	-0.003	-0.002	-0.004	0.065	0.044	0.021
C22	0.004	0.005	0.004	**0.113**	0.094	0.042
C23	-0.001	-0.002	-0.002	-0.039	-0.034	-0.034
C24	-0.001	-0.001	0.000	-0.016	-0.016	-0.011
C25	0.000	0.001	-0.001	-0.011	0.001	-0.011
C26	-0.001	-0.002	0.000	-0.009	-0.015	-0.004
C27	-0.001	-0.001	-0.001	-0.008	-0.011	-0.008

(b)

	f^-			f^+		
Atom	*Geo Opt*	*Equilibrium*		*Geo Opt*	*Equilibrium*	
		333 K	*353 K*		*333 K*	*353 K*
N1	0.010	0.036	0.066	0.001	0.009	0.015
C2	-0.017	-0.020	-0.031	-0.002	-0.011	-0.020
C3	-0.037	-0.045	-0.031	-0.009	-0.012	-0.020
N4	0.147	0.137	0.126	0.023	0.019	0.017
C5	-0.043	-0.037	-0.046	-0.008	-0.015	-0.028
C6	-0.038	-0.042	-0.025	-0.010	-0.016	-0.019
N7	**0.175**	**0.166**	**0.163**	0.117	0.128	0.141
C8	0.028	0.031	0.026	**0.168**	**0.140**	**0.159**
C9	-0.019	-0.017	-0.017	-0.009	-0.018	-0.019
C10	-0.012	-0.033	-0.014	-0.006	-0.012	-0.025
C11	-0.007	0.002	-0.005	-0.005	-0.006	-0.016
C12	-0.006	-0.009	-0.006	-0.003	-0.001	-0.008
C13	-0.004	-0.006	-0.001	-0.004	-0.005	-0.002
C14	-0.003	-0.008	-0.008	-0.004	-0.002	-0.008
C15	-0.002	-0.003	0.002	-0.006	-0.005	-0.001
C16	-0.002	-0.004	-0.004	-0.008	-0.005	-0.004
C17	-0.001	0.000	-0.004	-0.009	-0.010	-0.007
C18	-0.001	0.001	-0.002	-0.030	-0.017	-0.013
C19	0.000	0.000	0.000	-0.033	-0.022	-0.011
C20	-0.003	-0.004	-0.003	0.001	0.012	-0.007
C21	0.002	0.003	0.002	0.012	0.009	-0.002
C22	-0.002	0.000	-0.002	-0.045	-0.020	-0.007
C23	-0.001	0.000	-0.002	-0.020	-0.014	-0.011
C24	-0.001	-0.002	0.001	-0.013	-0.008	-0.003
C25	-0.001	-0.002	0.001	-0.006	-0.004	-0.001
C26	0.000	0.000	-0.001	-0.005	-0.003	-0.006
C27	-0.001	0.000	-0.002	-0.004	-0.003	-0.001
C28	0.001	0.000	0.001	-0.004	-0.003	-0.001
C29	0.001	0.001	-0.001	-0.003	-0.001	-0.002

4. Conclusion

In conclusion, the molecular dynamic simulation shows the change in the structure of the molecules at 333 K and 353 K, this is further proved by the changes in bond length from the geometry optimized structures to the equilibrium structures at 333 K and 353 K observed by each of the atoms in the molecules. The molecular dynamic simulation on the Fe surface also indicates that the imidazoline derivatives uses the imidazoline ring to effectively adsorb on the surface of iron at 333 K and 353 K. The quantum chemical calculation based on the natural atomic charge, the frontier molecular orbital and the Fukui indices values and plots shows the active sites of the molecules to be the N=C-N region in the imidazoline ring, the nitrogen and oxygen heteroatoms and the double bonded carbon atoms in the hydrophobic tail of the imidazoline derivative molecules. The quantum chemistry calculation also reveals that the pendent group in HNED and in NDDI which is attached to the imidazoline ring shows little HOMO and LUMO electron density and therefore the pendent group is not majorly involved in the donation of electrons in these molecules to the surface of Fe which can aid adsorption. There is no LUMO electron density seen in the pendent group, therefore the pendent group is not involved in the accepting of electrons from the d-orbital of the Fe atoms. The sites for electrophilic attack is shown to be mainly in the ring (mainly the N=C-N region) for the two molecules studied, while the sites for nucleophilic attack is shown to be in the ring for HNED, andthe double bonded carbon atoms in the alkyl hydrophobic tail for HNED and NDDI.The adsorption ability of the molecule is given as at geometry optimization; NDDI > HNED, at 333 K; NDDI > HNED and at 353 K; HNED > NDDI. But based from the geometry optimized structure NDDI has a better adsorption ability theoretically than HNED. The more comprehensive adsorption/inhibitive ability of the molecules obtained from the quantum chemical calculations is very much in line with the binding energies of the molecules to the Fe surface obtained from the molecular dynamic simulation at both temperatures studied.

5. Future Scope

We recommend that a thorough experimental research be carried out on these compounds, because theoretically it has shown to be a good corrosion inhibitor most especially for iron as well as petroleum pipelines. We also suggest that higher temperatures should be considered in studying the corrosion inhibitive/adsorption effect of these compounds. This study shows that the structural orientation of the atoms in a molecule can determine the adsorption/inhibitive ability of a particular molecule. Some new quantum chemical parameters were introduced in this work and can be looked into for further study for the adsorption/inhibitive effect of any molecule.

References

[1] H.Haixiang, D. Lie, L. Xiaochun, Z. Hongxia, Z. Xiuhui, S.Shumin,L. Hanlai, T. Xiaoyoung, Y.Jing,“ Experimental, quantum chemical and and molecular dynamics studies of imidazoline molecules against the

corrosion of steel and Quantitative Structure-Activity Relationship Analysis using the support vector machine (SVM) method," International Journal of Electrochemical Science, VIII, 11228-11247, 2013.

[2] M.S. El-Sayad, R.M. Erasmus, J.D.Comins, "In situ Raman Spectroscopy and electrochemical techniques for studying corrosion inhibition of iron in sodium chloride solution," Electrochimica Acta, LV,3657-3663, 2010.

[3] E. Khamis, N. Al- Andis, "Herbs as new type of green inhibitors for acidic corrosion,"Mater. Wissen. Werk, XXXIII,550-554,2002

[4] K.F.Khaled, "The Inhibition of benzimidazole derivatives on corrosion of iron in 1M HCl solutions, "Electrochimica Acta, XLVIII, 2493-2501, 2003

[5] S. Schauhoft, C.Kissel "New corrosion inhibitors for high temperature applications," Material and Corrosion,LI, 141-146, 1999

[6] .B. Obot, N.O. Obi-Egbedi, "Inhibitory effect and adsorption characteristics of 2,3-diaminonaphthalene at aluminium /hydrochloric acid interface:Experimrnt and theoretical study,"SurfaceReview and Letters, XV, 903-910, 2008.

[7] S.S. Abd El-Rehim, M.A. Ibrahim, F.F. Khaled, "4-Aminoantipyrine as an inhibitor of mild steel corrosion in HCl solution, Journal of Applied Electrochemistry, XXIX, 593-599, 1999

[8] N.O. Eddy, " Ethanol extract of PhyllanthusAmarus as a green inhibition for the corrosion of mild steel in H_2SO_4, Portugaliae Electrochimica Acta, XXVII, 579–589, 2009.

[9] S. Corona-Avendano, G. Alarcón-Ángeles, G.A. Rosquete-Pina, A. Rojas-Hernández, A. Gutiérrez,M. Ramírez-Silva, M. Romero- Romo, M. Palomar-Pardavé, " New insights on the nature of the chemical species involved during the process of dopamine deprotonation in aqueous solution: theoretical and experimental study, "Journal of Physical Chemistry, CXI, 1640, 2007.

[10] B. Gomez,N.V. Likhanov, M.A. Dominguez-Aguilar, R. Martinez-Palou, A. Vela, J.L.Gazquez,"Theoretical study of a new group of corrosion inhibitors, "Journal of Physical Chemistry, CX, 8928-8934, 2006

[11] Y. Tang, Y. Chen, W. Yang, Y. Liu, X. Yin,J. Wang, "Electrochemical and theoretical studies of thienyl-substituted amino triazoles on corrosion inhibition of copper in 0.5 M H_2SO_4," Journal of Applied Electrochemistry, XXXVIII, 1553-1559, 2008.

[12] P.Udhayakala, S. Rajendiran, S. Gunasekaran, "Quantum chemical studies on the efficiencies of vinyl imidazole derivatives as corrosion inhibitors for mild steel," Journal of Advanced Scientific Reasearch, III, 37-44, 2012.

[13] M.M. Kabanda, L.C. Murulana, M.Ozcan, F. Karadag, I. Dehri, I.B. Obot, E.E. Ebenso, "Quantum chemical studies on the corrosion inhibition of mild steel by some Triazoles and Benzimidazole Derivatives in acidic medium," International Journal of Electrochemical Science, VII, 5035-5056, 2012.

[14] J. Zhu, S. Chen, "A theoretical 1nvestigation on the inhibition efficiencies of some Schiff bases as corrosion inhibitors of steel in Hydrochloric acid," International Journal of Electrochemical Science, VII, 11884-11894, 2012.

[15] A. Zarrouk, I. El-Quali, M. Bouachrine, B. Hammouti, Y. Ramli, E.M. Essassi, I. Warad, A. Aounti, R. Salghi, " Theoretical approach to the corrosion inhibition efficiency of some Quinoxaline derivatives of steel in acid media using the DFT method," Research on Chemical Intermediates, XXXIX, 1125-1133, 2013.

[16] Y. Yan, W. Li, L. Cai, B.Hou, "Electrochemical and quantum chemical study of purines as corrosion inhibitors for mild steel in 1 M HCl solution," Electrochimica Acta, LIII, 5953–5960, 2008.

[17] A.Y. Musa, A.H. Kadhum, A.B. Mohamad, M.S. Takriff, "Experimental, theoretical study on the inhibition performance of triazole compounds for mild steel corrosion," Corrosion Science, 52, 3331–3340, 2010.

[18] A. Hassazadeh, " Inhibitor selection based on Nichols plot in corrosion studies," Electrochemica. Acta, LI, 305-316, 2004.

[19] Y.A. Musa, T.T. Ramzi, A.B. Mohamed, "Molecular dynamic and quantum chemical calculations for phthalazine derivatives as corrosion inhibitors of mild steel in 1M HCl," Corrosion Science, LVI, 176-183, 2012.

[20] B.Delley, Mordern density functional theory, Elsevier Science, Amsterdam, 2000.

[21] S. Xia, M. Qui, L. Yu, F. Lui, H. Zhao, "Molecular dynamics and density function theory study on relationship between structure of imidazoline derivatives and inhibition performance," Corrosion Sciences, L, 2012-2029. 2008.

[22] R.G. Parr, R.G. Pearson, "Absolute hardness: companion parameter to absolute electronegativity,"Journal of the America Chemical Society, CV, 7512-7516, 1983.

[23] R.G. Pearson, Inorganic Chemistry. Elsevier, Amsterdam,1988.

[24] H. Chermette, " Chemical reactivity indexes in density functional theory," Journal of Computational Chemistry, XX, 129-154, 1999.

[25] T.Koopmans,"Koopmans theorem in statistical Hartree-fock theory," Physica, I, 104-113, 1933.

[26] L. Pauling, The Nature of the Chemical Bond, Coruell University Press, New York, 1960.

[27] W. Yang, W. Mortier, "The use of global and local molecular parameters for the analysis of the gas phase basicity of amines," Journal of the America Chemical Society, CVIII, 5708-5713, 1986.

[28] P.C. Okafor, C.B. Liu, Y.J. Zhu, Y.G. Zheng, "Corrosion and corrosion inhibition behavior of N80 and P110 carbon steel in CO_2 saturated simulated formation water by rosin amide imidazoline. Industrial and Engineering Chemistry Research, L, 7273-7281, 2011.

[29] N. Roger, An introduction to surface chemistry. Queen Mary. London, 2006.

[30] B.Hellsing, Surface physics and Nano science physics. Goteborg University, Sweden,2008.

[31] A. Y. Musa, A.H. Kadhum, A.B. Mohamad, M.S. Takriff, "Molecular dynamic and quantum chemical calculation studies on 4,4-dimethyl-3-thiosemicarbazide

as corrosion inhibitor in 2.5 M H_2SO_4." Material Chemistry and Physics, CCXXIX, 660-665, 2011
[32] S.L. Li, Y.G. Wang, S.H. Chen, R. Yu, S.B. Lei, H.Y. Ma, D.X. Liu, "Some aspects of quantum chemical calculations for the study of Schiff base corrosion inhibitors on copper in NaCl solutions," Corrosion Science,XLI, 1769-1782, 1999.
[33] G. Gece, "The use of quantum chemical methods in corrosion inhibitor studies," Corrosion Science,L, 2981-2992, 2008.
[34] H. Ju, Z. Kai, Y. Li, " Aminic nitrogen-bearing polydentate Schiff base compounds as corrosion inhibitors for iron in acidic media: a quantum chemical calculation," Corrosion Science, L, 865-871, 2008.
[35] A. Yurt, S. Ulutasa, H. Dal, "Electrochemical and theoretical investigation on the corrosion of aluminium in acidic solution containing some Schiff bases," Applied Surface Science, 253,919-925, 2006.
[36] Z. Zhou, R.G.Parr,"Activation hardness: new index for describing the orientation of electrophilic aromatic substitution." Journal of America Chemical Society, CXII, 5720-5724, 1990.
[37] R. Hasanov, M. Sadikoglu and S. Bilgic, "Electrochemical and quantum chemical studies of some schiff base on the corrosion of steel in H_2SO_4 solution. Applied Surface Science, VIII, 3913, 2007.
[38] M. Fay, Chemistry 4th Ed, Pearson Education, New Jersey**,** 2004.
[39] V.F. Ekpo, P. C. Okafor, U.J. Ekpe and E.E. Ebenso, "Molecular dynamics simulation and quantum chemical calculations for the adsorption of some thiosemicarbazone (TSC) derivatives on mild steel. International Journal of Electrochemical Science, VI, 1045-1057, 2011.
[40] I.B. Obot, N.O. Obi-Egbedi, E.E. Ebenso, A.S. AfolabiandE.E. Oguzie, " Experimental, quantum chemical calculations and molecular dynamic simulation insight into the corrosion inhibition properties of 2-(6-methylpyridin-2-yl) oxazole [5,4-f][1,10]phenathroline on mild steel. Research on Chemical Intermdiates, XXXIX, 1927-1948, 2013.
[41] IUPAC, Compendium of Chemical Terminology, Electron Affinity, 2006.
[42] N.O. Obi-Egbedi, I.B. Obot,M.I. El-Khaiary, S.A. Umoren, E.E. Ebenso, "Computational simulation and statistical analysis on the relationship between corrosion inhibition efficiency and molecular structure of some phenathroline derivatives on mild steel surface,"International Journal of Electrochemical Science,VI, 5649-5675, 2011.
[43] I. Lukovits,E. Kalman, F. Zucchi, " Corrosion Inhibitors-correlation between electronic structure and efficiency,"Corrosion, LVII 3-8, 2001
[44] E. Stupnišek-Lisac, S. Podbrščck, T. Sorić, " Non-toxic organic zinc corrosion inhibitors in hydrochloric acid," Journal of Applied Electrochemistry, XXIV, 779–784, 1994.
[45] J.M. Roque, T. Pandiyan, J. Cruz, E,García-Ochoa, "DFT and electrochemical studies of tris(benzimidazole-2-ylmethyl)amine as an efficient corrosion inhibitor for carbon steel surface,"Corrosion Science, L, 614–624, 2008.

Author Profile

Kelechi Uwakwe holds a B.Sc. degree in Chemistry (2012) and an M.Sc. degree in Physical Chemistry (2016) from the University of Calabar, Calabar Nigeria. His research interests focus on corrosion studies and the reduction of CO_2 to CO using Computational Chemistry approach.

Obike Anthony Ikechukwu, has a Ph.D. in Physical Chemistry (2015) from The University of Calabar, Nigeria. He was a TWAS Scholar in 2011 and served at the renowned China Petroleum and Chemical Company (SINOPEC) as a Research Fellow from 2011 - 2012. He is currently a Lecturer in the Department of Pure and Industrial Chemistry, Abia State University. He is widely published in both local and international Journals. His research interest includes; Corrosion and Corrosion Inhibition, Bioremediation, Electrochemistry, Material Sciences and Nanotechnology.

Louis Hitler earned a B.S. degree in Industrial Chemistry from Federal University of Technology, Yola, Nigeria in 2014. In 2016, he was awarded a scholarship by the Chinese government to pursue his postgraduate studies at Institute of Nanoscience and Technology, Beijing, China. Louis is currently a full-time MSc. Candidate under the supervision of Professor He Tao at Nanocentre. Louis research focuses on computational techniques for characterizing the mechanisms and kinetics of heterogeneous catalytic reactions under realistic conditions. He is particularly interested in the applications of these approaches to study heterogeneous electrocatalysts for the conversion of carbon dioxide into industrially relevant chemical product and fuels.